Journal Title
XX(X):1–28

DOI: 10.1177/ToBeAssigned
www.sagepub.com/
SAGE

Assessment of the improvement of internal combustion engines cooling system using nanofluids and NePCM

Antonio J. Torregrosa[1], Alberto Broatch[1], P Olmeda[1] and Amin Dreif[1]

Abstract

In recent years, due to the increasing need to reduce consumption of reciprocating internal combustion engines, new researches on different subsystems have raised. Among them, the use of nanofluids as a coolant medium seems to be an interesting alternative. In this work, the potential benefits of using nanofluids in the cooling system by using an engine lumped model are studied. The methodology of the study starts with a whole description and validation of the model in both steady and transient conditions by means of a comparison with experimental results. Then the potential benefits that could be obtained with the use of nanofluids are studied in a theoretical way. After that, the model is used to estimate the behavior of the system by using different nanofluids in both stationary and transient conditions. The main results show that the advantages of using these new refrigerants are limited.

Keywords

Nanofluids, Heat transfer, Theoretical analysis, Engine Warm Up

[1]CMT-Motores Térmicos, Universitat Politècnica de València, Camino de Vera s/n. 46022 València, Spain

Corresponding author:
Pablo Olmeda, CMT-Motores Térmicos, Universitat Politècnica de València, Camino de Vera s/n. 46022 València, Spain
Email: pabolgon@mot.upv.es

Prepared using sagej.cls *[Version: 2017/01/17 v1.20]*

Introduction

Concerns about the efficient use of the available energetic resources have been a major issue for a long time, acquiring a central role after the energetic crisis of the seventies. Along with this motivation which led to big instability in the energetic supply and a high increase in fuel prices, in recent years, it has appeared a new one. Nowadays environmental concerns are widespread mainly due to two types of environmental problems arising from intensive use of fossil fuels: global scale effects (i.e. climate change) and local scale effects (i.e. poor air quality in cities). The combination of these aspects leads to scenarios with increasingly high fuel prices and stricter rules for its use, which directly affects the automotive industry. As the internal combustion engines dominate the automotive market, the efforts to raise their efficiency have been continuous. The research goes from the studies on new fuels[1] to improvements on engine subsystems as: new injection strategies, improvements in turbocharger models[2] or reducing heat losses improving the internal heat transfer[3].

The improvement of the engine cooling system is one of the solutions considered to face the increasingly strong requirements to the engines[4]. New cooling systems, more efficient and smaller, could get reductions in both fuel consumption and pollutant emissions. Possible improvements include the use of more complex systems of thermal management[5], which are able to adapt the refrigeration to the engine operating conditions and focus its efforts on critical areas of the engine, not wasting energy on those not as critical.

Regarding the raise of the engines efficiency, special attention should be given at their warming process[6]. During this stage the engines work below the design temperature which produces an increase in fuel consumption and pollutant emissions. Because of this, the minimization of its duration is one of the main objectives of the new thermal management systems. The importance of the warming process has even increased after hybrid automotive emergence in the market; since, in this kind of vehicles, intermittent operation of the combustion engine multiplies the number of these processes.

One of the studied options to reduce the warming duration is by using innovative refrigerant fluids, with better thermal properties. Choi[7] in 1995 at the Argonne National Laboratory (ANL) started the study of one of the most promising new kind of refrigerant which were coined nanofluids. The nanofluids consist in conventional refrigerants such as water, oil or mixtures of water and glycols where tiny solid particles (particles with a size smaller than 100 nm) are dispersed[8]. This addition is an attempt to improve fluid thermal properties by taking advantage of the generally higher thermal conductivity of the solids.

Most studies performed about nanofluids have pointed out a noticeable increase of their thermal conductivity compared to conventional fluids[9]. This feature results in higher heat transfer coefficients[10] enabling the use of less coolant flows[11]. On the contrary, wall shear stress values for nanofluids is greater than that of the base liquid[12]. Additionally, nanofluids have a smaller specific heat due to the lower nanoparticles material specific heat; which together with the use of less coolant flows would, in principle, shorten engine heating times. Furthermore it could be mentioned other potential benefits of use nanofluids as, for instance, reducing the size and weight of

the cooling system. That, in turn, would bring reductions in fuel consumption and free up space to address new more aerodynamic designs or hybrid powertrains architecture.

The study of the use of nanofluids on internal combustion engines is very limited: a numerical study on the effect of nanofluids on the warm-up time of an engine has been studied in [13] where a reduction of this time is observed. Kulkarni et al. [14] used nanofluids in a cogeneration system and the results showed an increase on heat exchanger efficient due to higher heat transfer coefficient but a decrease on the cogeneration efficient due to the lower heat capacity of the mixture with nanofluids.

Due to all the mentioned possible advantages, this work proposes an assessment of the applicability of nanofluids as coolants of a car engine by means of the use of a lumped model. This model simulates the temperature distribution in the block, piston and head-cylinder of the engine in function of the operating conditions. The lumped model was validated with empirical data from temperature measurements both in steady and transient conditions. Summarizing, the objective of this paper is the evaluation of the potential improvements in fuel consumption (reduction of CO_2) and hence in efficiency of an IC automobile engine cooling system due to the use of nanofluids as coolants.

The content of the paper is organized as follows. First, a description of the engine thermal model is presented where its general geometry and boundary conditions are briefly explained. After that, the model validation both in steady and transient state is presented. Then, the way how thermophysical nanofluids properties were computed as well as the specific nanoparticles and base fluids chosen and their properties are described. The expressions to compute the effects of nanoparticles addition on pressure drop and convective heat transfer coefficient are developed. Once the main theory is introduced, it is explained the general methodology and cases studied in the work. Finally, the results for each of the cases studied are presented and the most relevant conclusions drawn from the work are outlined.

Engine Thermal model

In order to assess the possible advantage of the nanofluids as engine coolants, a modified model of the one developed in [15] has been employed. The main modifications introduced in this work are the following:

- a higher discretization, i.e. an increase of the number of nodes in which the engine geometry is divided.
- the division of the coolant flow into nodes to make its thermal balance more accurate.
- the use of a new correlation to determine the heat transfer coefficient between the material nodes and the coolant.

The lumped model represents the engine as a thermal mesh which consists in a finite number of nodes. Inside each node the conduction thermal resistance is neglected so they will be on internal thermal equilibrium, i.e. without inside thermal gradients. The different nodes are joined by thermal resistances computed according to the kind of

contact between them. Moreover the nodal thermal capacitance is taken into account as function of its mass and specific heat.

By applying the first principle of thermodynamics to each node, a set of simultaneous equations, which allows the calculation of the temperature distribution for each operation conditions, are obtained. Once the temperature distribution is known the determination of thermal flows between nodes is straightforward. Equation 1 shows the resulting equation for the structural nodes.

$$m_i\, c \left(\frac{T^i_{t+\Delta t} - T^i_t}{\Delta t} \right) = \sum_j \frac{k_{ij}\, A_{ij}}{d_{ij}} \left(T^j_{t+\Delta t} - T^i_{t+\Delta t} \right) + \sum_k \dot{Q}_{k \to i} + \sum_l h_{li}\, A_{li} \left(T^l_{t+\Delta t} - T^i_{t+\Delta t} \right) \tag{1}$$

The temperatures from the right hand side of the Equation 1 are evaluated at the instant $t + \Delta t$ (implicit method) in order to ensure the model stability when transient processes are simulated. In addition, the energy balance of the coolant nodes is shown in Equation 2 where the temperature of each node is computed as the arithmetic mean between the inlet and outlet.

$$\frac{m_i\, c_p}{\Delta t} \left(\frac{T^{i,ou}_{t+\Delta t} + T^{i,in}_{t+\Delta t}}{2} - \frac{T^{i,ou}_t + T^{i,in}_t}{2} \right) + \dot{m}_i\, c_p \left(T^{i,ou}_{t+\Delta t} - T^{i,in}_{t+\Delta t} \right) = \sum_k \dot{Q}_{k \to i} + \sum_i h_{ij}\, A_{ij} \left(T^j_{t+\Delta t} - \frac{T^{i,ou}_{t+\Delta t} + T^{i,in}_{t+\Delta t}}{2} \right) \tag{2}$$

Geometrical node division

In order to use the lumped capacitance model in different engines and to reduce the calculation times a simplified geometry of an engine has been used. This simplification takes into account the most usual geometries for the piston, cylinder-head and liner and they are related to the main geometrical characteristics of an engine as piston diameter, stroke or compression ratio, valves diameters. Then, the simplified geometry was divided into different nodes according to the localization of the biggest thermal gradients and the location of the thermocouples used in the experimental validation[16]. The nodes in each of the elements has been chosen as follows:

- The cylinder is divided into five axial nodes, two radial and six circumferential, adding another line of nodes outside of the top of the cylinder, in such a way that the first axial level has three radial levels. Consequently, the cylinder has 66 nodes as shown in Figure 1.
- The piston is divided into ten nodes with azimuthal symmetry as shown in Figure 2.

- Undoubtedly the division of the head-cylinder is the hardest one due to its complicated geometry and its large amount of components. Because of this the head-cylinder is simplified taking into account only the main components with plain shapes. The number of used nodes in this case is 35, a scheme of their distribution is shown in Figure 3.

- Finally, the coolant has been divided in several nodes in order to improve the accuracy of its thermal balance. First, the coolant is split in two main paths: one passing through the liner and the other flowing through the cylinder-head. Besides, each of these two main paths, the coolant is divided in different nodes:

  – The coolant which crosses the head-cylinder is divided in two nodes, one in contact with the intake area and another with the exhaust area.

  – The coolant which crosses the cylinder is divided in four axial levels and five circumferential. The coolant has one circumferential node less than the cylinder because one of the circumferential columns of nodes in the cylinder is considered insulated because it has no contact with the coolant and it is in contact with an analogous node of the next cylinder, this one corresponds with the first circumferential nodes of the Figure 1. The coolant division scheme is shown in Figure 4.

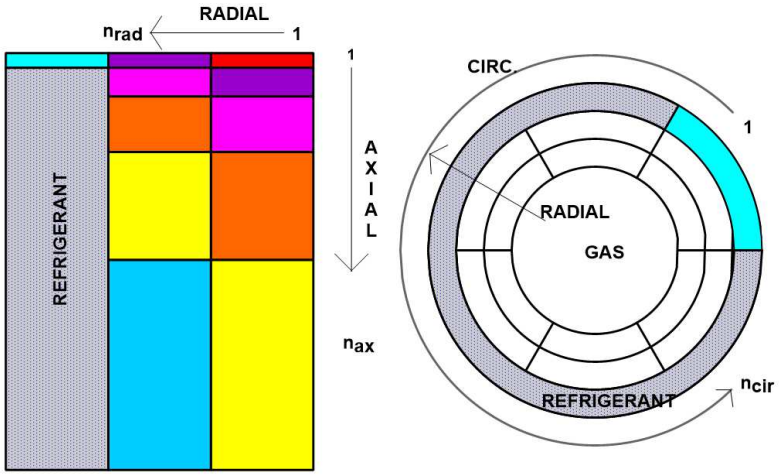

Figure 1. Position of cylinder nodes

Consequently, the total number of metallic nodes is 111 while there are 22 different coolant nodes. The rest of the boundary conditions are: lubricating oil, in-cylinder gases, inlet air and exhaust gases. These boundary conditions are characterized by their average temperatures and film coefficients. These are the only boundary conditions considered in the model, i.e. other possible boundary conditions as external surfaces

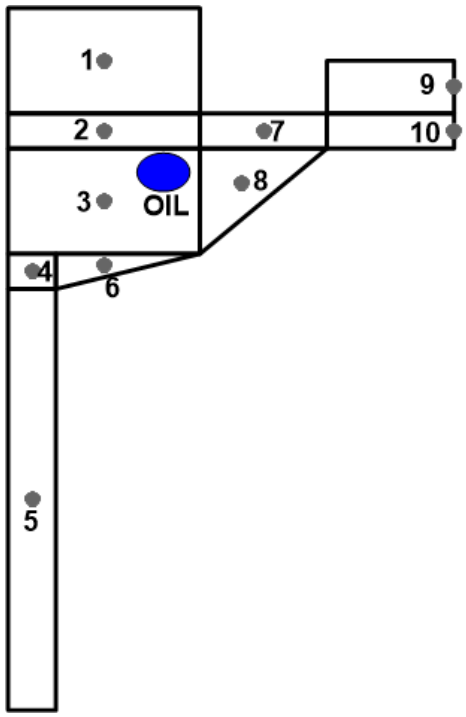

Figure 2. Position of nodes in the piston

are neglected. As remarked in [15], a quasi-steady state analysis of the combustion process in the combustion chamber and of the flows in the inlet and outlet ducts is considered. With that goal, average values of the parameters which characterize the former processes are taken throughout the cycle. A summary of how the boundary conditions are modelled is presented below. Further details are provided in [15].

Coolant-wall heat transfer

In the interaction between the coolant nodes and the liner nodes and between the coolant nodes and the cylinder-head nodes a modification was introduce in order to take into account the operating running conditions in the film coefficient calculation. First, as mentioned before, the coolant flow was split into two identical parts; one of them flowing through the cylinder block while the other flowing through the cylinder-head. Then, the coolant velocities for each path are calculated, which are used to compute the Reynolds number. The coolant convective heat transfer coefficient is different in each of the considered paths due to the different geometry:

- In the case of the liner, a modification of the Grimison correlation [17] for a bank of tubes, see Equation 3, was applied, where b_1 and b_2 are constants depending on the distance between the cylinders, and b_3 is a constant which corrects the

correlation for the case of banks with less than ten rows of tubes (in this case only one tube).

$$Nu = 1.13\, b_1\, b_3\, Re_{D,max}^{b_2}\, Pr^{\frac{1}{3}} \tag{3}$$

- For the cylinder-head the Dittus-Boelter correlation [18], see Equation 4, was used.

$$Nu = 0.023\, Re^{0.8}\, Pr^{0.4} \tag{4}$$

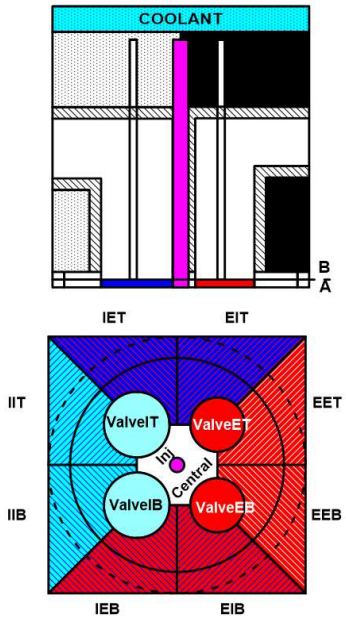

Figure 3. Position of nodes in cylinder head

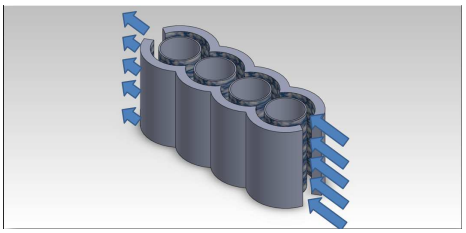

Figure 4. Coolant nodal division in the liner and head-cylinder.

Model validation

Steady state validation

As it was explained in the previous section, in order to validate the lumped model a set of experimental measurements were used. These measurements were carried out over an engine whose features are summarized in Table 1.

Table 1. Features of the used engine in the validation of the lumped model

Parameter	Value
Displacement	1600 cm^3
Number of cylinders	4
Diameter	0.075 m
Stroke	0.088 m
Bowl diameter	0.04635 m
Compression ratio	17

Several thermocouples were placed in the engine, each of these correspond with a structural node of the lumped model. The thermocouple logged the temperature evolution in several operation conditions. The data from the thermocouples were compared with the model predictions; some of the results are presented in Figure 5. The speed and load conditions for the different test carried out are summarized in Table 2. After looking at the plots in the Figure 5 it can be seen how the model predictions correspond fairly well to the experimental data obtained.

Table 2. Tests performed for steady state validation

Test name	Speed [rpm]	bmep [bar]	Test name	Speed [rpm]	bmep [bar]
1	1500	4.9	7	3000	3.1
2	2000	3.2	8	3000	6.6
3	2000	7.3	9	3000	11.8
4	2000	11.6	10	3500	2.6
5	2500	2.2	11	3500	4.7
6	2500	7.0	12	4000	3.7

Transient validation

In order to validate the model in transient simulations it was checked the correspondence between the experimental data and the predicted results when the engine underwent a sudden change. To carry out these comparisons the engine was set in a constant speed and load conditions and then it was applied a sudden change in one of the parameters, keeping the other constant. For instance, Figure 6 show the results for the changes occurred when, with the engine running at 2000 rpm and 6.54 bar of bmep, the load is raised until 18.77 bar keeping the speed constant.

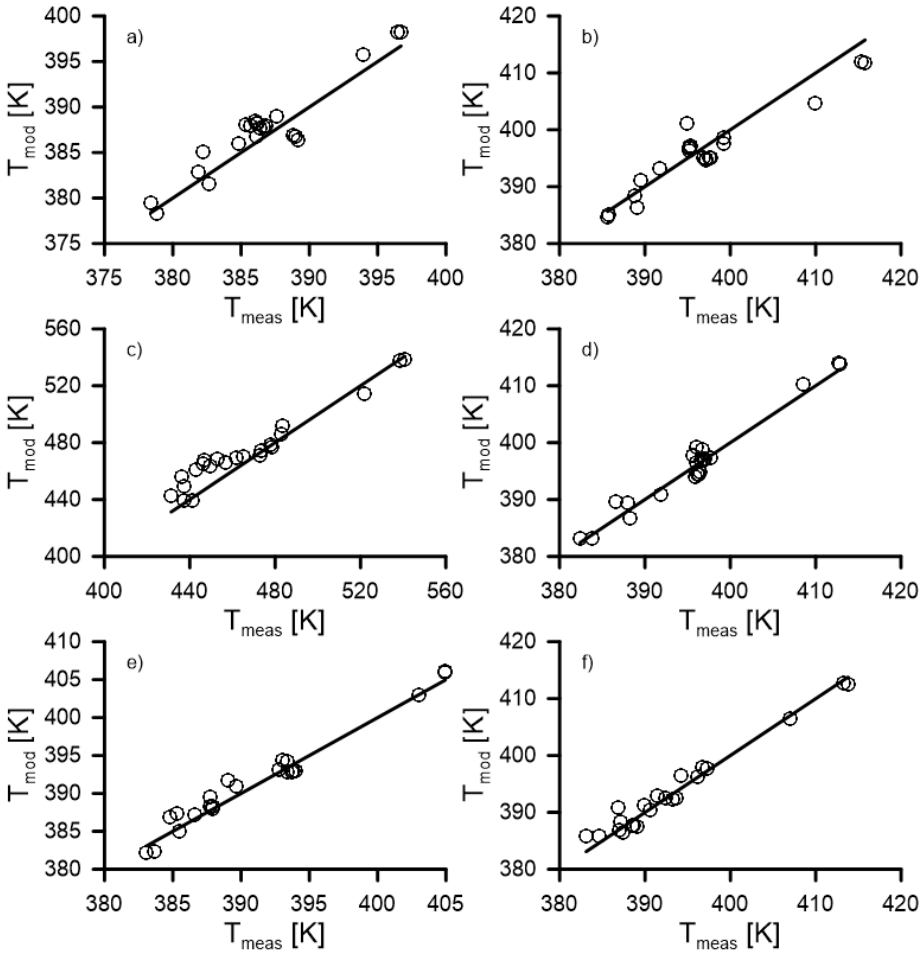

Figure 5. Predicted versus measured temperatures in cylinder 1: a) Exhaust side at 8 mm, b) Injector hole exhaust side at 8.7 mm, c) Cylinder 1 bowl rim , d) Exhaust valve seat at 3.5 mm, e) Intake valve seat at 3.5 mm f) Admission side at 3.5 mm

Figure 6 shows a good agreement between the predicted results by the model and the experimental data obtained in the engine characterized in Table 1. Accordingly, a good quality of the results using nanofluids could be expected in order to evaluate its suitability as coolant fluids in the engine.

Thermophysical properties of nanofluids

In order to compute the thermophysical properties of mixtures between coolants and nanoparticles the following formulas were used:

- Density: The studies about nanofluid density are quite limited and, in general, it is used the mixture theory[19]:

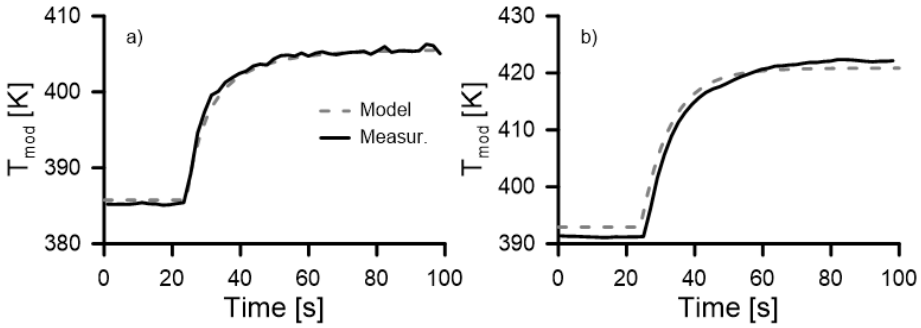

Figure 6. Predicted versus measured temperatures in cylinder 1: a) Exhaust side at 8 mm, b) Intake valve seat at 3.5 mm

$$\rho_{nf} = (1-\phi)\ \rho_b + \phi\,\rho_p \tag{5}$$

- Specific heat: As in the case of density, studies about nanofluid specific heat are limited and they generally use the thermal equilibrium[19]. The specific heat capacity of a nanofluid with NePCMs should take into account the contribution of the latent heat of the core of the NePCM. In this way, the specific heat capacity of the nanofluid, c_{nf}, is obtained by:

$$\begin{aligned} c_{nf} = & \frac{(1-\phi)\ \rho_b\, c_b + \phi\,\rho_p\, c_p}{(1-\phi)\ \rho_b + \phi\,\rho_p} \\ & + \frac{H_{NePCM}\phi}{\Delta T/_3} sin\left(\frac{T - T_{onset}}{\Delta T/_3}\right) \end{aligned} \tag{6}$$

  where the first term takes into account the contribution of the specific heat of the NePCM using the mixing rule and the second term takes into account the latent heat contribution of the NePCM cores. In the second term, H_{NePCM}, T_{onset} and ΔT are the phase change enthalpy, onset temperature and characteristic temperature width of the NePCM. The second term only contributes from T_{onset} to $(T_{onset} + \Delta T)$.

- Thermal conductivity: The thermal conductivity is one of the most important features of nanofluids since the most positive effects of the nanoparticle addition are presented. This fact has led to a widely researches in the open bibliography, where several models have been proposed in order to explain and predict its behaviour. However, a general agreement has not been reached due to the high variety of results found in the literature. Nevertheless, there seems to be agreement on the general trend which indicates an important increase in the thermal conductivity with the nanoparticle addition. One of the main theory is based on the formation of liquid nanolayers around the nanoparticles which explains the increase in thermal conductivity. In this paper, the Yu and Choi correlation[20], Equation 7, has been chosen to predict the thermal conductivity

of the mixture. It must be remarked that the mentioned correlation is based on the one proposed by Maxwell[21] by taking into account the existence of the mentioned nanolayers, i.e. using a conductivity for the equivalent nanoparticles that is shown in Equation 8.

$$k_{nf} = \frac{k_{pe} + 2\,k_b + 2\,(k_{pe} - k_b)\,(1+\beta)^3\,\phi}{k_{pe} + 2\,k_b - (k_{pe} - k_b)\,(1+\beta)^3\,\phi} k_b \tag{7}$$

$$k_{pe} = \frac{\left[2\,(1-\gamma) + (1+\beta)^3\,(1+2\,\gamma)\right]\gamma}{-(1-\gamma) + (1+\beta)^3\,(1+2\,\gamma)} k_p \tag{8}$$

The main problem of Equations 7 and 8 lay on the fact that no experimental data is allowable to predict nor nanolayer thickness δ neither nanolayor thermal conductivity k_l. In order to fulfil this problem, a simplified case where the thermal conductivity of the equivalent nanoparticles and single nanoparticles are equal has been considered as it has been proposed in Mansour[22], where the ratio of nanolayer thickness and nanoparticle radio was considered constant and equal to 0.1. With these hypotheses, the predicted thermal conductivities will be slightly bigger than those predicted by the exact model. However, the deviations observed in low concentrations of nanoparticles (as the ones used in this work) are negligible.

- Viscosity: As in the previous cases, the diversity of results and models concerning nanofluids viscosity is fairly high. For this reason it was decided to use one of the benchmark model, established as reference in the majority of work on this subject. This is the one presented by Einstein in 1906[23]. This model is applicable to very dilute suspensions of hard spherical particles, and neglects the interaction between the particles. Its expression is given in Equation 9.

$$\mu_{ef} = \mu_f\,(1 + 2.5\,\phi) \tag{9}$$

The thermophysical properties of both the water-ethylene mixture and the nanofluid are presented on Table 3.

Table 3. Thermophysical properties of the nanofluids components

Component	ρ [kg m^{-3}]	c [kJ kg K^{-}1]	k [W m^{-}1 K^{-}1]	μ 10^{-}6 [Pa s]
Water - Ethylene glycol 40 %	1011	3840	0.53	680.5
Nanoparticles (TiO_2)	4200	520	21.9	-

Overall, this model underestimates the experimental results obtained for nanofluids so it must be expected a too optimistic analysis by using it[24–26]. This will be taken into account when defining the conclusions. In Figure 7 it can be observed that density, thermal conductivity and viscosity are higher

as the nanoparticule concentration increase due to the intrinsic properties of the nanoparticule. On the other hand, the specific heat increases with the concentration because of the latent heat absorbed by the PCM core.

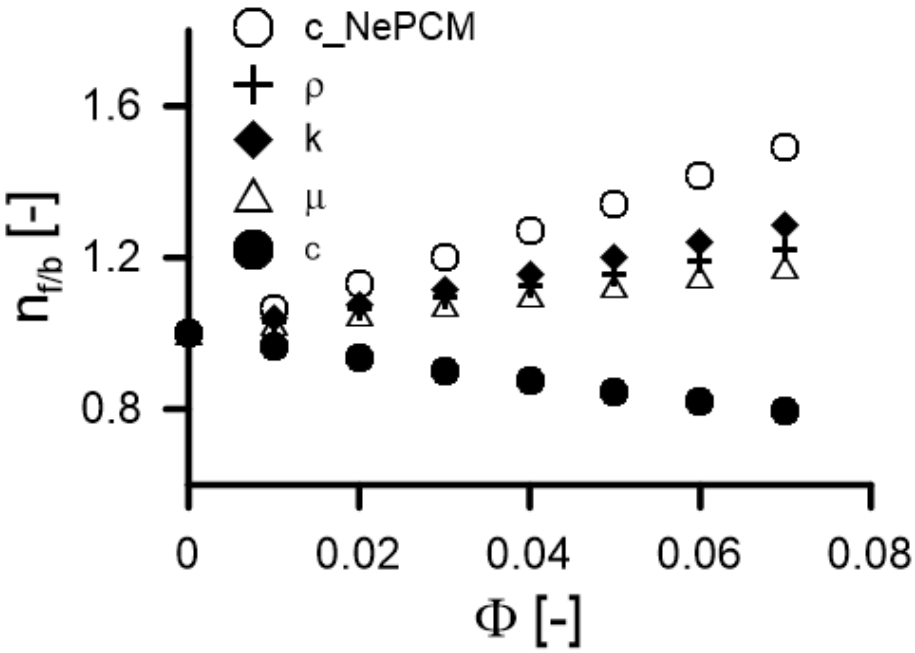

Figure 7. Ratio between nanofluid and base fluid properties and its dependence of the nanoparticle concentration

Effects of the nanofluids on pressure drop and convective heat transfer coefficient

The effect on pressure drop and convective heat transfer coefficient due to the change on the thermophysical properties of the mixtures of a base fluid with nanoparticles will be outlined. The comparison between the behaviour of the refrigeration with nanofluids versus with regular coolants, will be performed assuming:

- As.1. The same correlations are applicable for heat transfer and friction coefficients in both cases: standard coolant and nanofluids.
- As. 2. The geometry of the engine is not changed.

Effects on heat transfer coefficient

The variation of the convective heat transfer coefficient in an engine will be analyzed assuming that forced convection can be estimated with Equation 10 which is the same

as Equation 4. This equation can be used since no specific correlation for nanofluids has been found to be valid[27] and therefore classic correlations must be used[28]:

$$Nu = b_4\, Re^{b_5} \cdot Pr^{b_6} \tag{10}$$

Choosing correctly the fitting coefficients of Equation 10, the Dittus-Boelter correlation[18] is obtained, which its accuracy in predicting the heat transfer coefficient in nanofluids has been demonstrated by[19]. The fitting cooefficients are shown in Equation 4. The expressions of the dimensionless numbers of Equation 10 are presented in Equations 11, 12 and 13.

$$Re = \frac{\rho u D}{\mu} = \frac{4\,\dot{m}}{\pi\,\mu\,D} \tag{11}$$

$$Pr = \frac{\mu\, c}{k} \tag{12}$$

$$Nu = \frac{h\, D}{k} \tag{13}$$

Using assumptions 1 and 2, the ratios between Reynolds numbers (Equation 11) and Prandtl numbers (Equation 12) are presented in Equations 14 and 15 respectively.

$$\frac{Re_{nf}}{Re_b} = \left(\frac{\rho_{nf}}{\rho_b}\right)\left(\frac{u_{nf}}{u_b}\right)\left(\frac{\mu_{nf}}{\mu_b}\right)^{-1} \tag{14}$$

$$\frac{Pr_{nf}}{Pr_b} = \left(\frac{\mu_{nf}}{\mu_b}\right)\left(\frac{c_{nf}}{c_b}\right)\left(\frac{k_{nf}}{k_b}\right)^{-1} \tag{15}$$

The relationship between the film coefficients with and without nanofluids, which is the appropiate simple figure of merit for comparing the forced single-phase convective heat transfer performance of a nanofluid relative to its base fluid[19], is presented in Equation 16 that has been obtained combining equations 10 13, 14 and 15.

$$\frac{h_{nf}}{h_b} = \left(\frac{Re_{nf}}{Re_b}\right)^{b_5}\left(\frac{Pr_{nf}}{Pr_b}\right)^{b_6}\left(\frac{k_{nf}}{k_b}\right) \tag{16}$$

Effects on pressure drop

The effect of nanofluids on pressure can represent a change on the power consumed by the coolant pump that can be calculated using Equation 17, where the pressure drop ΔP can be computed with the expression 18.

$$\dot{W}_b = \Delta P\, \dot{V} \tag{17}$$

$$\Delta P = f\frac{\rho\, u^2}{2\, D} L \tag{18}$$

The friction factor in Equation 18 is calculated using 19.

$$f = \begin{cases} 0.316\, Re^{-1/4} & \text{if } Re \leq 2 \cdot 10^4 \\ 0.184\, Re^{-1/4} & \text{if } Re > 2 \cdot 10^4 \end{cases} \tag{19}$$

Then, using Equations 17 and 18, the relationship between powers consumed by the coolant pump are obtained as Equation 20.

$$\frac{\dot{W}_{nf}}{\dot{W}_b} = \frac{\Delta P_{nf}}{\Delta P_b} \frac{\dot{V}_{nf}}{\dot{V}_b} = \left(\frac{f_{nf}}{f_b}\right) \left(\frac{\rho_{nf}}{\rho_b}\right) \left(\frac{u_{nf}}{u_b}\right)^3 \tag{20}$$

Equation 20 can be simplified assuming that the change of the coolant will not affect the flow regime as Equation 21 shows. This will not always be true and it could lead to changes in the results but, only in particular conditions the assumption will be false. Equation 22 show the result of applying this last assumption, where the fitting constants depend on Reynolds number according to Equation 19..

$$\begin{aligned} Re_{nf} \leq Re_b \leq 2 \cdot 10^4 \\ Re_b > Re_{nf} > 2 \cdot 10^4 \end{aligned} \tag{21}$$

$$\frac{\dot{W}_{nf}}{\dot{W}_b} = \left(\frac{Re_{nf}}{Re_b}\right)^{-b_7} \left(\frac{\rho_{nf}}{\rho_b}\right) \left(\frac{u_{nf}}{u_b}\right)^3 \tag{22}$$

Methodology

For the present study, two different cases (constant volumetric flow and constant wall temperature) are considered for comparison among three different coolants; base fluid, nanofluid and nanofluid with NePCM. These cases have been chosen in order to estimate the possible gains on heat transfer keeping the same flow and to estimate the possible gains on coolant flow (power) by keeping the same heat transfer conditions.

Case 1

The first case considered is assuming that the volumetric flow remains constant in both systems (regular coolant and with nanofluids) as Equation 23 shows. In this case, the ratios between the Reynolds numbers (Equation 14) and ratio between coolant pump power (Equation 22) can be simplified. These simplifications lead to Equation 24 and 25 respectively.

$$\dot{V}_{nf} = \dot{V}_b \longrightarrow u_{nf}\, A_{nf} = u_b\, A_b \xrightarrow{As.2} u_{nf} = u_b \tag{23}$$

$$\frac{Re_{nf}}{Re_b} = \left(\frac{\rho_{nf}}{\rho_b}\right) \left(\frac{\mu_{nf}}{\mu_b}\right)^{-1} \tag{24}$$

$$\frac{\dot{W}_{nf}}{\dot{W}_b} = \left(\frac{Re_{nf}}{Re_b}\right)^{-b_7} \left(\frac{\rho_{nf}}{\rho_b}\right) \tag{25}$$

Figure 8 and Figure 9 show the variation of several parameters with the nanoparticle concentration for this specific case, where the following trends were observed:

- The effect of nanofluids concentration on Reynolds number is small, but in any case the higher the concentrarion, the higher the Reynolds number. This is explained since the increase of density with nanofluids concentration is higher than the increase of the dynamic viscosity (as Figure 7 show).
- The ratio of Prandtl numbers is highly dependent on the nanofluids concentration and decreases with nanofluid concentration. This is because of the fact that the increase in the ratio of conductivities is higher than the one observed for the dynamic viscosity. Additionally, the ratio of specific heat capacities decreases with nanofluids concentration as it is shown in Figure 7. On the other hand, the ratio of specific heat capacities increases with nanofluids concentration as it is shown in Figure 7 due to the strong effect of the second term of the Equation 6 as long as the nanofluid operates within the designed temperature range. Thus, this effect will be available just for a certain temperature range in which the melting point of the PCM is achieved.
- On one hand, the ratio of Nusselt number decreases with concentration when using nanofluids. This is a consequence of the two previous statements: ratio of Reynolds number is almost constant and the ratio of Prandtl numbers decreases. This result could lead to the wrong idea (as it will be shown later) that the heat transfer using nanofluids would be lower than the one obtained with the base fluids. On the other hand, the results with NePCM showed that Nusselt number increased as a consequence of Prandtl number increase.
- The effect in convective heat transfer coefficient is very important: increases with nanofluid concentration. This effect is explained since the increase of thermal conductivity is much important than the decrease of the Nusselt number. This result confirms that the appropiate simple figure of merit for comparing the heat transfer performance of a nanofluid relative to its base fluid is the convective heat transfer coefficient and not the Nusselt number as stated by [19]. For the case of nanofluid with NePCM the same trend was observed but the film coefficient increase was much higher.
- The trend observed in the friction factor is opposite and lower than the one observed for the Reynolds number as expected since this factor depends only on Reynolds number as Equation 19 shows.
- The high increase observed in the coolant pump power is due to the low effect of nanoparticles in Reynolds number and the high effect that they have on density (see Figure 7).

Case 2

In this second case, the wall temperatures are kept constant. This fact implies that the heat transferred to coolant is kept constant, so the relationship presented in Equation 26 holds.

$$\dot{Q}_{nf} = \dot{Q}_b \longrightarrow h_{nf} = h_b \tag{26}$$

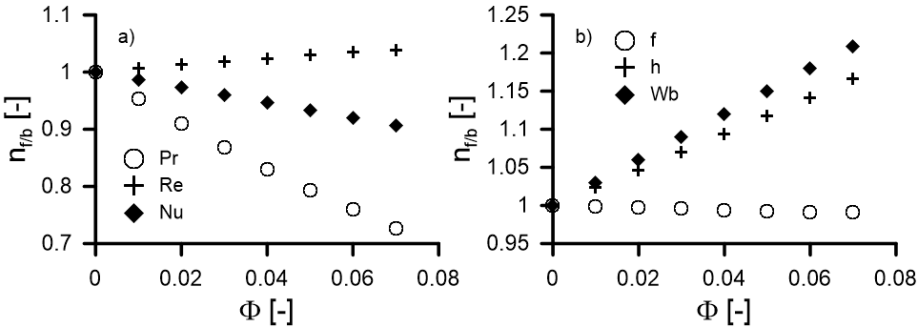

Figure 8. Ratio between nanofluid and base fluid properties and its dependence on the nanoparticle concentration for case 1: a) Ratio of Prandtl, Reynolds and Nusselt numbers, b) film coefficient, friction factor and pumping power ratios

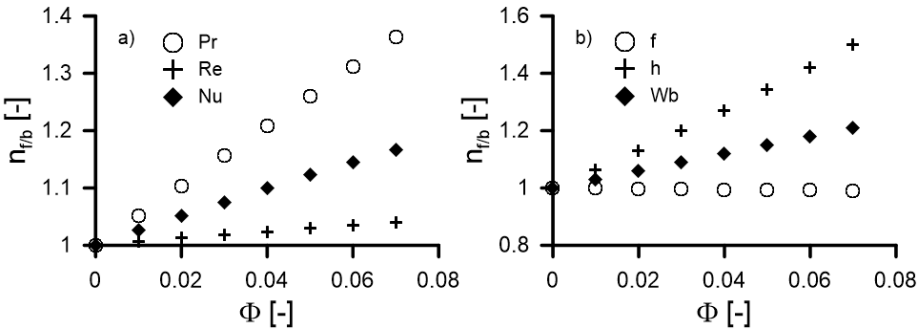

Figure 9. Ratio between NePCM nanofluid and base fluid properties and its dependence on the nanoparticle concentration for case 1: a) Ratio of Prandtl, Reynolds and Nusselt numbers, b) film coefficient, friction factor and pumping power ratios

Applying a similar methodology using different ratios will be obtained. First, the ratio between the Reynolds number can be obtained by combining Equations 16, 26 and 26. The result is presented in Equation 27.

$$\left(\frac{Re_{nf}}{Re_b}\right)^{b_5} = \left(\frac{Pr_{nf}}{Pr_b}\right)^{-b_6} \left(\frac{k_{nf}}{k_b}\right)^{-1} \tag{27}$$

In order to obtain the ratio between the coolant pump powers for this specific case, the ratio between velocities is needed. This velocities ratio (Equation 28) can be obtained by using the definition of Reynolds number (Equation 11) and the ratio between Reynolds numbers for this specific case (Equation 27). Now, the ratio between coolant pump powers is easily obtained, whose expression can be found in Equation 29

$$\frac{u_{nf}}{u_b} = \left(\frac{Re_{nf}}{Re_b}\right) \left(\frac{\rho_{nf}}{\rho_b}\right)^{-1} \left(\frac{\mu_{nf}}{\mu_b}\right) \tag{28}$$

$$\frac{\dot{W}_{nf}}{\dot{W}_b} = \left(\frac{Re_{nf}}{Re_b}\right)^{3-b_7} \left(\frac{\rho_{nf}}{\rho_b}\right)^{-2} \left(\frac{\mu_{nf}}{\mu_b}\right)^{3} \tag{29}$$

Figure 10 and Figure 11 show the variation of several parameters with the nanoparticle concentration for this specific case, where the following trends are observed:

- The effect of nanofluids concentration on Reynolds number is more important than for case 1 and following the opposite trend, i.e. the higher the concentrarion, the lower the Reynolds number. This is explained since the increase of density with nanofluids concentration is higher than the increase of the dynamic viscosity (as Figure 7 shows)
- The effect on Prandtl number is the same as the one observed in the previous section since Prandtl number depend only on thermophysical propertes.
- The decrease of Nusselt number is higher than the observed in case 1 due to, on one hand, the same bahaviour in Prandtl number and, on the other, the observed behaviour on Reynolds number. However, when using NePCM nanoparticles the trend compared with the case 1 changes due to the decrease of both Prandtl and Reynolds numbers with nanoparticle concentration.
- There is no effect in convective heat transfer coefficient due to the constant wall temperature approach.
- The trend observed in the friction factor is opposite and lower than the one observed for the Reynolds number as explaneid in the previous case.
- The decrease (opposite to the observed behaviour of case 1) observed in the coolant pump power is due to the fact that the decrease in Reynolds number and the increase of densities (the power is inversely proportional to this densities ratio as Equation 29 show (see Figure 7) are more important than the increase on dynamic viscosity. The same behaviour is observed when using NePCM nanoparticle is similar but with higher decrease in pumping power. This is because the Reynolds number is even lower with this nanoparticle.

Summarizing, Table 4 and Table 5 show, in approximate way , the effect of the nanofluid concentration on the different parameters in each of the considered case. The numerical values indicates the approximate expected variation of the parameter respect a variation of 1 $\%$ increase on nanofluid concentration.

Results

Case 1 (Constant $\dot{V}$). Steady state

As mentioned, in this case, the coolant volumetric flow remains constant and, as a consequence, higher heat transfer coefficients are obtained with nanofluids respect to base fluid leading to an increase of the heat transferred to the coolant. The results obtained with the lumped model with different nanofluid concentrations for all the

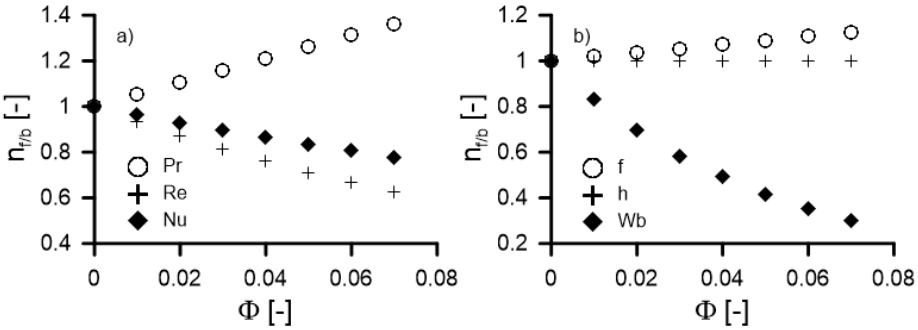

Figure 10. Ratio between nanofluid and base fluid properties and its dependence of the nanoparticle concentration for case 2: a) Dimensionless numbers, b) film coefficient, friction factor and pumping power

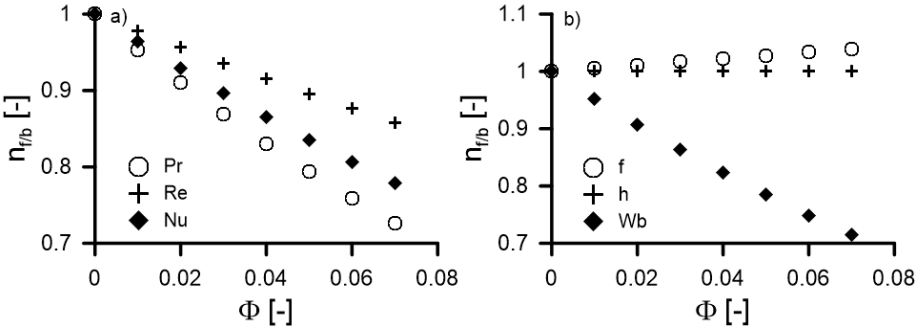

Figure 11. Ratio between NePCM nanofluid and base fluid properties and its dependence of the nanoparticle concentration for case 2: a) Dimensionless numbers, b) film coefficient, friction factor and pumping power

Table 4. Approximate variation of the different parameters respect to nanofluid concentration

Parameter	Case 1 Constant volumetric flow rate	Case 2 Constant heat transfer
u	0	-2.4
Re	0.55	-2.0
Pr	-3.8	-3.8
Nu	-1.3	-3.1
h	2.4	0
f	-0.12	0.50
$\dot{W}_b$	3.0	-4.0

steady state engine working conditions are presented in Figure 12, where an increase

Table 5. Approximate % variation of the different parameters respect to NePCM nanofluid concentration

Parameter	Case 1 Constant volumetric flow rate	Case 2 Constant heat transfer
u	0	-6.9
Re	0.55	-5.2
Pr	5.2	5.2
Nu	2.2	-3.1
h	7.1	0
f	-0.12	1.3
$\dot{W}_b$	3	-9.2

around 18% of the convective heat transfer coefficient (which correspond of a 7% of nanoparticle concentration) leads to an increment of only 1.3% in the heat transferred to the coolant.

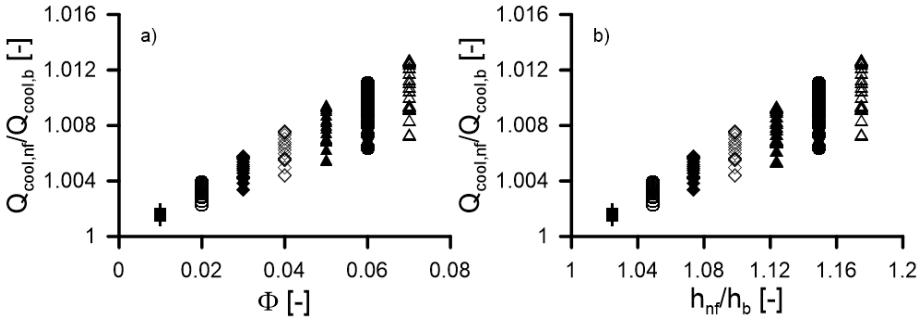

Figure 12. Relationship between heat transferred to the coolant depending on a) nanoparticle concentration and b) film coefficients

On the other hand, when using NePCM a similar behaviour was observed. In Figure 13 it is seen that the heat rejected to the coolant in this case was slightly higher (2.3% compared to base coolant) while the convective heat coefficient achieved an increment of 35% for the case of high load and speed (test 9 in Table 2) and 7% of NePCM nanoparticle concentration. In addition, Figure 13 shows that when NePCM are used the results obtained for each test differ more than the previous case because of the second term of Equation 6 which depends on the coolant temperature. Thus, the higher the coolant temperature rise when passing through the engine the higher the convective heat coefficient because of the fact that the heat rejected is absorbed for the coolant as latent heat. This effect could be beneficial in engine downsizing strategy because less coolant volume would be required and detrimental for warm up of the engine as it will be seen in the following section.

The explanation of this results come from the fact that the main thermal resistance in the heat transfer between in-cylinder gases and coolant is the convective coefficient

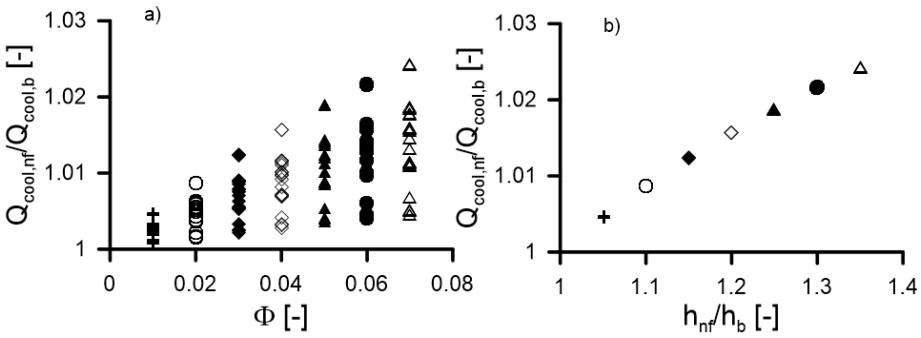

Figure 13. Relationship between heat transferred to the coolant depending on a) NePCM nanoparticle concentration and b) film coefficients

between gas and combustion chamber wall. This small gain will not be enough to compensate the higher power consumed by the coolant pump.

Case 1 (Constant $\dot{V}$). Transient

In order to study the suitability of the use of nanofluids through transient processes, a simulation with the lumped model is performed. This simulation has been performed with the engine running at 2000 rpm and 6.54 bar of bmep, the load is raised until 18.77 bar keeping the speed constant.. The obtained results are presented in Figure 14, which shows that the higher nanoparticle concentration has the coolant, the lower the temperatures at which the structure nodes are stabilized. This is because the increment in the nanoparticle concentration leads to a higher convective heat transfer coefficient, as it can be seen in Figure 8.

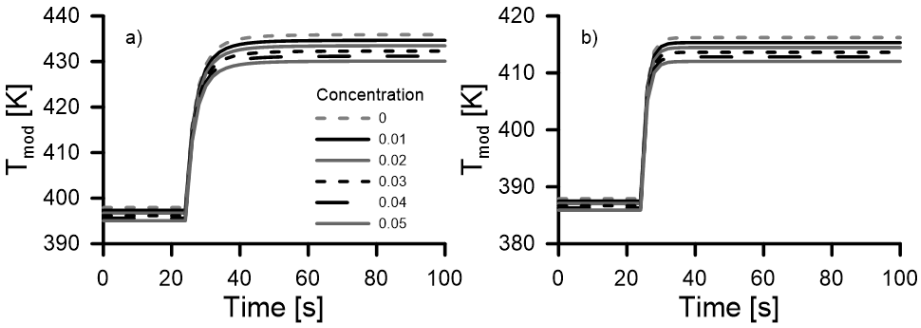

Figure 14. Temperature evolution during a transient process with different particle concentrations in cylinder 1: a) Exhaust side at 8 mm, b) Intake valve seat at 3.5 mm

The results obtained with NePCM are shown in Figure 15. The warm up time is quite similar to the case without NePCM but the final temperature is lower (around 4 K for the case of 5% nanoparticle concentration) compared to the previous case for both studied points, exhaust side and intake valve seat. This was expected due to the fact

that the heat capacity is higher in this case. Additionally, there is a difference in warm up time between them due to their thermal inertia which is lower for the intake valve seat.

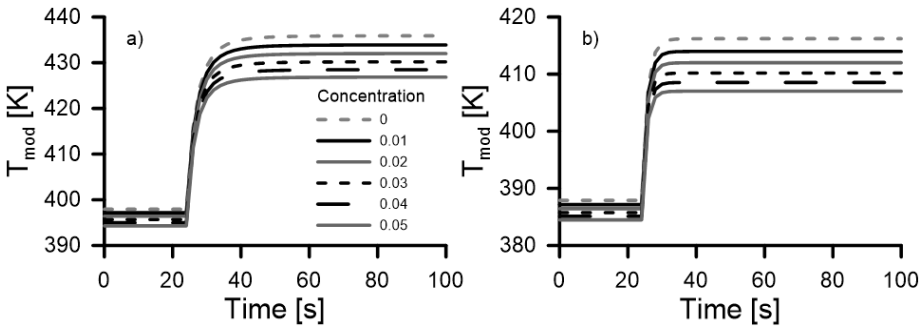

Figure 15. Temperature evolution during a transient process with different NePCM particle concentrations in cylinder 1: a) Exhaust side at 8 mm, b) Intake valve seat at 3.5 mm

The warming time (that could lead to a reduction on fuel consumption[6]) is not significantly affected by the use of nanofluids in these given conditions.

Case 2 (Constant $\dot{Q}$). Steady state

As indicated previously, in this case, the heat transferred to the coolant was kept constant, so the advantage of using nanofluids could come from the reduction of the coolant flow allowed by the improved film coefficient of the nanofluids. This flow reduction leads to power consumption savings in the coolant pump (as Equation 30 shows).

$$\dot{W}_{nf} = \frac{\Delta P \dot{V}}{\eta} \tag{30}$$

The pressure drop is directly proportional to the square of the volumetric flow rate. The constant of proportionality was determined from experimental data measured as Equations 31 and 32 show.

$$\Delta P = b_8 \cdot \dot{V}^2 \tag{31}$$

$$b_8 = 5.14 \cdot 10^{-5}\ bar\, l^{-2}\, min^2 \tag{32}$$

Besides, the coolant pump is usually fitted to the engine crankshaft as, a consequence, the coolant volumetric flow rate is almost proportional to the engine speed, so Equation 33 can be used it. As above, the constant of proportionality was determined from experimental data measured (Equation 34).

$$Q = b_9 \cdot n \tag{33}$$

$$b_9 = 3.631 \cdot 10^{-2}\ l\, min^{-1}\, rpm^{-1} \tag{34}$$

Finally, for the usual coolant pumps used in internal combustion engines, the coolant pump performance is bounded between 0.85 and 0.9 so, conservatively, a value of 0.85 was taken in the simulations.

By combining Equations 30 to 34, the pumping power is calculated as a function of engine speed as shown in Equation 35.

$$\dot{W}_b = 2.89483 \cdot 10^{-9} \cdot n^3 \tag{35}$$

Finally, to have an idea of the relative importance of this power (and the possible savings obtained) with the use of nanofluids, a comparison with the engine effective power will be performed. The obtained results are shown in Figure 16.

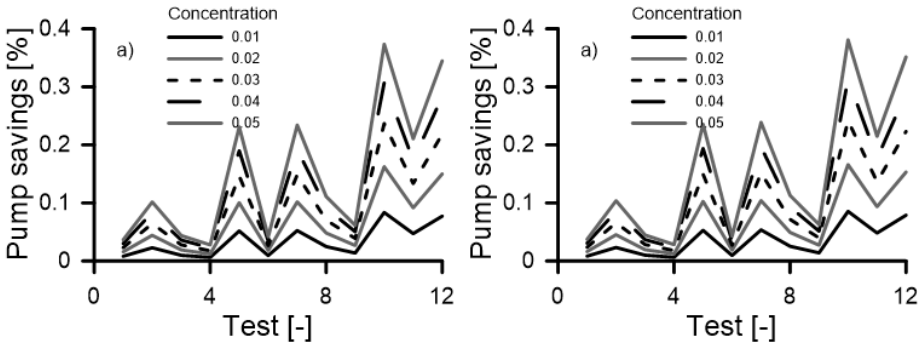

Figure 16. Power saved at the pump related to engine effective power: a) Re $\leq 2 \cdot 10^{-4}$, b) Re $> 2 \cdot 10^{-4}$

As it can be seen, using nanofluids leads to a limited savings in the power consumed by the coolant pump if the engine effective power is taken into account. The maximum percentage values are around 0.4 $\%$ for the highest nanoparticles concentrations evaluated. These small savings cannot possibly justify the use of these new coolants since they possibly have adverse effects (for instance, instability and bigger environmental impacts) and higher costs (maintenance).

Case 2 (Constant $\dot{Q}$). Transient

In this specific case, the study of the transient process does not give any additional information since the refrigeration is kept constant. The only parameter that would vary is the volumetric flow rate.

WLTC cycle simulation

In order to evaluate the effect in engine performance under more demanding conditions a WLTC cycle was simulated when nanofluid is used as coolant. Furthermore, it is a very dynamic cycle with diverse operating conditions which serve as a realistic scenario for assessing the real potential of nanofluid cooling strategy.

In the simulation, the NePCM nanofluid was not used due to the wide range of coolant temperature during the cycle. This would require a specific study for each particular NePCM with its own fusion temperature.

Contrary to the previous cases, for the WLTC simulation, the coolant volumetric flow and heat flux were not restrained. Figure 17 shows the results obtained simulating the cycle starting from ambient conditions (20C).

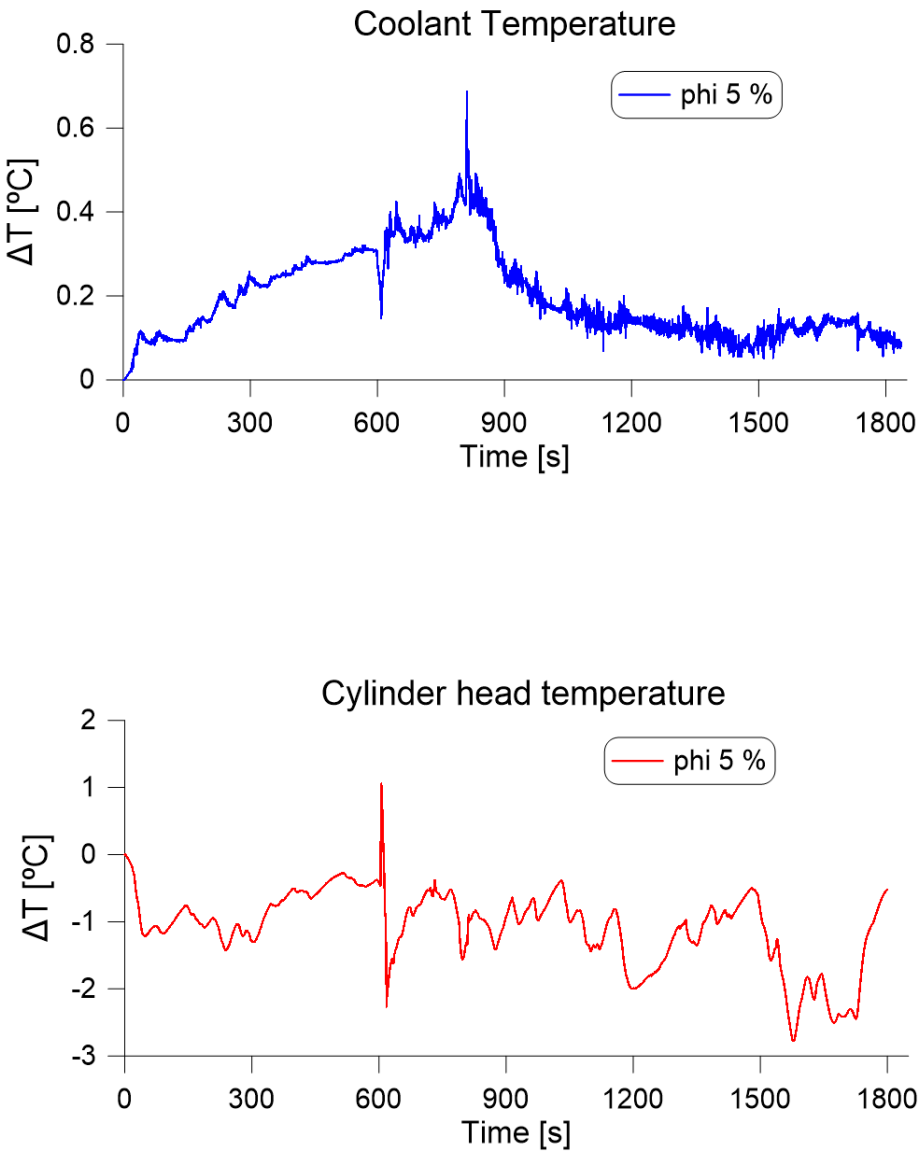

Figure 17. Coolant and cylinder head temperature (Intake valve seat at 3.5 mm) difference during a WLTC cycle starting from ambient conditions.

On one hand, the plot at the top represents the coolant temperature difference in the engine outlet between the case of 5% nanoparticle concentration and base

fluid. A positive value means that the temperature of the coolant is higher with the concentration. It can be seen that the maximum temperature difference is around 0.6C. Regarding the warm up reduction time (temperature of the coolant above 80C), it is practically negligible as it can be deduced by the plot.

On the other hand, the bottom plot shows the temperature difference in the cylinder head for the same nanoparticle concentration. It can be seen that the nanoparticle concetration in the coolant decreases the material temperature during all the cycle reaching a minimum value of -2.7C. After 600s there is a short period of time in which the behavior seems to be different from the rest of the cycle (temperature of the material rises with the concentration). This is due to the switching from HPEGR to LPEGR by the control system when a certain coolant temperature is reached. For the case of 5% nanoparticle concetration this temperature is reached sooner increasing the intake air mass of the engine in those few instants.

Conclusions

A theoretical study about the potential suitability of using nanofluids as engine coolants has been performed followed by numerical simulations.

- The evaluation of the thermal effects were carried out by using a lumped thermal model to predict the heat flux distribution over an engine in many different operation conditions in steady state and transient conditions.

- The main features of the model have been explained as well as the validation procedure. The results obtained confirmed the reliability of the model.

- It was quantified the variation in the nanofluid thermophysical properties with nanoparticle concentration. In order to assess the increase in the heat transfer and pump loses two cases were studied. On one hand, the volumetric flow was set constant and, on the other hand, the heat transfer coefficient was kept constant. In the study, it was evaluated the effect of including NePCM in the nanoparticle. This NePCM nanofluid increased the film heat transfer coefficient compared to the normal nanofluid. In this case, it was assumed that equations for the thermophysical properties were the same as with normal nanoparticle. Additionally, it should be taken into account that the thermal conductivity and viscosity models used to predict nanofluids properties are too optimistic. The largest errors are expected in the calculation of viscosity, as experimental studies show that this model predicts much lower viscosities than those measured. Although, the Einstein model was chosen for the sake of simplicity and for the lack of a reliable general model. Furthermore, it should be noted that several hypotheses were made. For instance, it was assumed that the same correlations are applicable to nanofluids and that the flow regime remains constant having changed the coolant.

- The results obtained showed very little improvements in engine operation through all the cases studied. In steady state conditions, although the heat transfer coefficient increased around 25% for the case of maximum nanoparticle

concentration, the heat flux only increased in approximately 1.3%. The calculations for the case with NePCM showed the same behavior with an increment of 50% in the heat transfer coefficient and 2.3% in the heat flux. Regarding the pump savings, the results showed less than 0.5% for 5% of nanoparticle concetration. In transient conditions, the concentration of nanoparticle decreased the temperature at which the material is thermally steadied. Finally, a WLTC cycle was performed and demonstrated the limited effects in the engine thermal performance.

In addition to the limited benefits of using nanofluids, there is the fact that applying this type of coolants in real engines would mean more investment in maintenance and manufacturing costs because of the presence of metal nanoparticles in the coolant circuit which could accumulate in some parts and plug the circuit as well as reduce the life of the coolant pump.

Acknowledgments

The equipment used in this work has been partially supported by FEDER project funds Dotacin de infraestructuras cientfico tcnicas para el Centro Integral de Mejora Energtica y Medioambiental de Sistemas de Transporte (CiMeT) [grant number FEDER-ICTS-2012-06], framed in the operational program of unique scientific and technical infrastructure of the Spanish Government.

References

1. Broatch A, Tormos B, Olmeda P et al. Impact of biodiesel fuel on cold starting of automotive direct injection diesel engines. *Energy* 2014; 73: 653–660.
2. Payri F, Olmeda P, Arnau FJ et al. External heat losses in small turbochargers: Model and experiments. *Energy* 2014; 71: 534–546.
3. Broatch A, Olmeda P, García A et al. Impact of swirl on in-cylinder heat transfer in a light-duty diesel engine. *Energy* 2017; 119: 1010–1023.
4. Burke RD, Lewis AJ, Akehurst S et al. Systems optimisation of an active thermal management system during engine warm-up. *P I Mech Eng D-J Aut* 2012; 226(10): 1365–1379.
5. Torregrosa AJ, Broatch A, Olmeda P et al. Experiments on subcooled flow boiling in I.C. engine-like conditions at low flow velocities. *Exp Therm Fluid Sci* 2014; 52: 347–354.
6. Torregrosa AJ, Broatch A, Olmeda P et al. Assessment of the influence of different cooling system configurations on engine warm-up, emissions and fuel consumption. *Int J Automot Techn* 2008; 9(4): 447–458.
7. Choi SUS. Enhancing thermal conductivity of fluids with nanoparticles. In *ASME International Mechanical Engineering Congress & Exposition, November 12-17,1995, San Francisco, CA.*, volume 231. pp. 99–105.
8. Daungthongsuk W and Wongwises S. A critical review of convective heat transfer of nanofluids. *Renew Sust Energ Rev* 2007; 11(5): 797–817.
9. Tavman I, Turgut A, Chirtoc M et al. Experimental Study on Thermal Conductivity and Viscosity of Water-Based Nanofluids. *Heat Transf Res* 2010; 41(3): 339–351.

10. Kakaç S and Pramuanjaroenkij A. Review of convective heat transfer enhancement with nanofluids. *Int J Heat Mass Tran* 2009; 52(13-14): 3187–3196.
11. Özerinç S, Kakaç S and YazIcIolu AG. Enhanced thermal conductivity of nanofluids: A state-of-the-art review. *Microfluid Nanofluid* 2010; 8(2): 145–170.
12. Bianco V, Chiacchio F, Manca O et al. Numerical investigation of nanofluids forced convection in circular tubes. *Appl Therm Eng* 2009; 29(17-18): 3632–3642.
13. Vila Millan M and Samuel S. Nanofluids and thermal management strategy for automotive application. In *SAE Technical Paper 2015-01-1753*.
14. Kulkarni DP, Vajjha RS, Das DK et al. Application of aluminum oxide nanofluids in diesel electric generator as jacket water coolant. *Appl Therm Eng* 2008; 28(14-15): 1774–1781.
15. Torregrosa AJ, Olmeda P, Martín J et al. A tool for predicting the thermal performance of a diesel engine. *Heat Transfer Eng* 2011; 32(10): 891–904.
16. Torregrosa A, Olmeda P, Degraeuwe B et al. A concise wall temperature model for di Diesel engines. *Appl Therm Eng* 2006; 26(11-12): 1320–1327.
17. Incropera FP, Dewitt DP, Bergman TL et al. *Fundamentals of Heat and Mass Transfer*. 6th ed. John Wiley & Sons, 2007.
18. Dittus FW and Boelter LM. Heat transfer in automobile radiators of the tubular type. *Int Commun Heat Mass* 1985; 12(1): 3–22.
19. Yu W, France DM, Timofeeva EV et al. Comparative review of turbulent heat transfer of nanofluids. *Int J Heat Mass Tran* 2012; 55(21-22): 5380–5396.
20. Yu W and Choi SU. The role of interfacial layers in the enhanced thermal conductivity of nanofluids: A renovated Hamilton-Crosser model. *J Nanopart Res* 2004; 6(4): 355–361.
21. Maxwell JC. *A treatise on electricity and magnetism*, volume I. Oxford University Press, 1873.
22. Mansour RB, Galanis N and Nguyen CT. Effect of uncertainties in physical properties on forced convection heat transfer with nanofluids. *Appl Therm Eng* 2007; 27(1): 240–249.
23. Einstein A. A new determination of molecular dimensions. *Annalen de Physik* 1906; 19(4): 289–306.
24. Duangthongsuk W and Wongwises S. Measurement of temperature-dependent thermal conductivity and viscosity of TiO2-water nanofluids. *Exp Therm Fluid Sci* 2009; 33(4): 706–714.
25. Kole M and Dey TK. Viscosity of alumina nanoparticles dispersed in car engine coolant. *Exp Therm Fluid Sci* 2010; 34(6): 677–683.
26. Chandrasekar M, Suresh S and Chandra Bose A. Experimental investigations and theoretical determination of thermal conductivity and viscosity of Al2O3/water nanofluid. *Exp Therm Fluid Sci* 2010; 34(2): 210–216.
27. Sarkar J. A critical review on convective heat transfer correlations of nanofluids. *Renew Sust Energ Rev* 2011; 15(6): 3271–3277.
28. Murshed SM, Nieto De Castro CA, Loureno MJ et al. A review of boiling and convective heat transfer with nanofluids. *Renew Sust Energ Rev* 2011; 15(5): 2342–2354.

Appendix

Nomenclature

A	Area	m^2
b	Weighting factor	$-$
c	Specific heat capacity	$J \cdot kg^{-1} \cdot K^{-1}$
c_m	Mean piston velocity	$m \cdot s^{-1}$
c_u	Tangential velocity	$m \cdot s^{-1}$
d	Distance between nodes	m
D	Bore, Diameter	m
f	Friction factor	$-$
h	Convective coefficient	$W \cdot m^{-2} \cdot K^{-1}$
L	Length	m
k	Thermal conductivity	$W \cdot m^{-1} \cdot K^{-1}$
m	Mass	kg
$\dot{m}$	Mass flow rate	$kg \cdot s^{-1}$
n	Engine speed	rpm
Nu	Nusselt number	$-$
p	Pressure	Pa
Pr	Prandtl number	$-$
$\dot{Q}$	Heat flow	W
Re	Reynolds number	$-$
t	Time	s
T	Temperature	K
u	Velocity	$m \cdot s^{-1}$
V	Displacement, volume	m^{-3}
$\dot{V}$	Volumetric flow rate	$m^{-3} \cdot s^{-1}$
$\dot{W}$	Power	W
PCM	Phase Change Material	$-$
$NePCM$	NanoEcapsulated Phase Change Material	$-$
$WLTC$	Worldwide harmonized Light vehicles Test Cycles	$-$
Greeks symbols		
α	Crank angle	$\circ$
β	Angular width	$\circ$
β	ratio of nanolayer thickness and nanaparticle radio	$-$
δ	Thickness	m
Δ	Increment	
η	Efficiency	$-$
γ	Ratio of nanolayer and nanoparticle conductivities	$-$
μ	Dynamic viscosity	$Pa \cdot s$
ν	Kynematic viscosity	$m^2 \cdot s^{-1}$
ϕ	Proportion	$-$
ρ	Density	$kg \cdot m^-3$
Subscripts and superscripts		
0	Motored	

b	Base
con	Contact
g	Gas
i	Component
IVC	Intake valve closing
in	Inlet
j	Component
k	Component
l	Component
lin	Refers to liner
nf	Nanofluid
oil	Refers to oil
ou	Outlet
p	Particle
pe	Equivalent nanoparticle
pis	Refers to piston
ru	Runner
s	Segment
T	Total
u	Tangential
w	Wall